A&A 561, A42 (2014)
DOI: 10.1051/0004-6361/201322273

Astronomy & Astrophysics

Molecules in the transition disk orbiting T Chamaeleontis⋆

G. G. Sacco[1], J. H. Kastner[2], T. Forveille[3], D. Principe[2], R. Montez Jr.[4], B. Zuckerman[5], and P. Hily-Blant[3]

[1] INAF – Osservatorio Astrofisico di Arcetri, Largo E. Fermi 5, 50125 Firenze, Italy
e-mail: gsacco@arcetri.inaf.it
[2] Center for Imaging Science and Laboratory for Multiwavelength Astrophysics, Rochester Institute of Technology, 54 Lomb Memorial Drive, Rochester NY 14623, USA
[3] Laboratoire d'Astrophysique de Grenoble, Université Joseph Fourier-CNRS, BP 53, 38041 Grenoble Cedex, France
[4] Department of Physics and Astronomy, Vanderbilt University, Nashville, TN 37235, USA
[5] Department of Physics and Astronomy, University of California, Los Angeles, CA 90095, USA

Received 13 July 2013 / Accepted 24 October 2013

ABSTRACT

Aims. We seek to establish the presence and properties of gas in the circumstellar disk orbiting T Cha, a nearby ($d \sim 110$ pc), relatively evolved (age ~5–7 Myr) yet actively accreting 1.5 $M_\odot$ T Tauri star.
Methods. We used the Atacama Pathfinder Experiment (APEX) 12 m radiotelescope to search for submillimeter molecular emission from the T Cha disk, and we reanalyzed archival *XMM-Newton* imaging spectroscopy of T Cha to ascertain the intervening absorption due to disk gas along the line of sight to the star ($N_{\rm H}$).
Results. We detected submillimeter rotational transitions of ^{12}CO, ^{13}CO, HCN, CN, and HCO$^+$ from the T Cha disk. The ^{12}CO line (and possibly the ^{13}CO line) appears to display a double-peaked line profile indicative of Keplerian rotation; hence, these molecular line observations constitute the first direct demonstration of the presence of cold molecular gas orbiting T Cha. Analysis of the CO emission line data indicates that the disk around T Cha has a mass ($M_{\rm disk,H_2} = 80\ M_\oplus$) similar to, but more compact ($R_{\rm disk,CO} \sim 80$ AU) than other nearby, evolved molecular disks (e.g., V4046 Sgr, TW Hya, MP Mus) in which cold molecular gas has been previously detected. The HCO$^+$/^{13}CO and HCN/^{13}CO line ratios measured for T Cha appear similar to those of other evolved circumstellar disks (i.e., TW Hya and V4046 Sgr). The CN/^{13}CO ratio appears somewhat weaker, but due to the low signal-to-noise ratio of our detection, this discrepancy is not strongly significant. Analysis of the *XMM-Newton* X-ray spectroscopic data shows that the atomic absorption $N_{\rm H}$ toward T Cha is one to two orders of magnitude larger than toward the other nearby T Tauri with evolved disks, which are seen at much lower inclination angles. Furthermore, the ratio between atomic absorption and optical extinction $N_{\rm H}/A_V$ toward T Cha is higher than the typical value observed for the interstellar medium and young stellar objects in the Orion nebula cluster. This may suggest that the fraction of metals in the disk gas is higher than in the interstellar medium. However, an X-ray absorption model appropriate for the physical and chemical conditions of a circumstellar disk is required to address this issue.
Conclusions. Our results confirm that pre-main-sequence stars older than ~5 Myr retain cold molecular disks when accreting, and that those relatively evolved disks display similar physical and chemical properties.

Key words. protoplanetary disks – submillimeter: stars – stars: pre-main sequence – stars: individual: T Cha

1. Introduction

Circumstellar disks serve both as sources of material for accreting stars and as the sites of nascent planetary systems. Observations that can establish the physical conditions and evolution of the gaseous components of such disks are essential to understand the accretion process and the processes involved in planet formation. Observation of emission lines from molecular species (e.g., CO, HCN, CN, HCO$^+$) in the submillimeter represents a powerful tool for studying cold (10–100 K) gas located in the outer regions ($R > 10$ AU) of circumstellar disks. Submillimeter observations of molecular emission from disks orbiting young stars have been carried out in the last two decades, using both single dish and interferometric facilities; many of these studies have focused on relatively evolved pre-main-sequence (pre-MS) star/disk systems that are located away from dark clouds and, hence, are free of potential contaminating cloud CO line emission (e.g., Dutrey et al. 1994, 1997, 2008; Kastner et al. 1997, 2008; Thi et al. 2004; Qi et al. 2004, 2006, 2008; Piétu et al. 2007; Rodriguez et al. 2010; Öberg et al. 2010, 2011; Andrews et al. 2012, and references therein).

In the last few years, our group initiated a campaign of multiwavelength observations of young, roughly solar-mass pre-MS stars within ~100 pc that are still accreting gas from their circumstellar disks. Only four pre-MS stars (TW Hya, V4046 Sgr, MP Mus, and T Cha), all located in the southern hemisphere, are known to share all of these properties. Thanks to their proximity and ages, these stars are particularly suitable for studies of star and planet formation processes: they are close enough for detailed study of the spatial structure of their disks with high spatial resolution facilities; they are old enough (ages ~5–20 Myr) that their disks may already have spawned giant protoplanets; and their disks still retain significant amounts of gas, as demonstrated by signatures of stellar accretion in the optical through

⋆ Based on submillimeter and X-ray observations. Submillimeter observations have been collected at the European Organisation for Astronomical Research in the Southern Hemisphere, Chile, with the Atacama Pathfinder Experiment APEX (Prog. ID 088.C-0441 and E-089.C-0518A). X-ray archival observations used in this paper have been obtained with *XMM-Newton*, an ESA science mission with instruments and contributions directly funded by ESA member states and NASA.

X-ray regimes (e.g., Alencar & Batalha 2002; Argiroffi et al. 2012; Curran et al. 2011).

The archetype of these young stars is TW Hya. The presence of molecular gas orbiting TW Hya was first established via single-dish CO observations by Zuckerman et al. (1995); subsequently, its disk has been scrutinized via both single-dish molecular line surveys (Kastner et al. 1997; Thi et al. 2004) and interferometric imaging (Qi et al. 2004, 2006, 2008; Hughes et al. 2011; Rosenfeld et al. 2012b). More recently, we detected molecular emission from disks orbiting two additional nearby, accreting pre-MS stars, V4046 Sgr, and MP Mus (Kastner et al. 2008, 2010). Like TW Hya, the former system has been investigated in multiple molecular tracers (Kastner et al. 2008; Öberg et al. 2011) and has been mapped interferometrically (Rodriguez et al. 2010; Öberg et al. 2011; Andrews et al. 2012; Rosenfeld et al. 2012a), whereas thus far the MP Mus molecular disk has only been detected via single-dish spectroscopy of ^{12}CO. Given simple assumptions concerning disk CO abundance, the CO submillimeter emission and continuum observations of the dust suggest gas-to-dust ratios close to unity for all three disks, suggesting either that these disks have already depleted a large part of their primordial gas (as initially proposed by Dutrey et al. 1997) or that the [CO]/H_2 number ratio is much smaller than the value of 10^{-4} usually adopted for purposes of estimating molecular gas masses from CO data. Furthermore, certain radio molecular lines measured for V4046 Sgr and TW Hya suggest that the chemistry of the circumstellar gas is influenced by the strong high-energy (UV and/or X-ray) radiation fields of the stars (Kastner et al. 2008; Salter et al. 2011).

Our target T Cha is a K0 V star of 1.5 $M_\odot$ that is likely a member of the ϵ Chamaeleontis Association, on the basis of its kinematic properties (Torres et al. 2008; Olofsson et al. 2011; Murphy et al. 2013). Kinematic data have been used to derive the distances to the Association and its members, with two recent studies finding distances in the range 107–110 pc, both to the Association and T Cha itself (Torres et al. 2008; Murphy et al. 2013). Hence, in this paper, we adopt the distance of 110 pc to T Cha. The age of the Association is more uncertain. Torres et al. (2008) proposed an age of 6–7 Myr, while Murphy et al. (2013) recently suggested a younger age (3–5 Myr). According to its position in the HR diagram relative to theoretical pre-MS sequence evolutionary tracks, T Cha appears to be older than the rest of the Association (10–12 Myr from Kastner et al. 2012; and Murphy et al. 2013). However, Murphy et al. (2013) argue that evolutionary models imply ages for solar mass stars that are older than their actual ages due to a systematic error in the models or in inferred values of temperature and luminosity. Furthermore, T Cha is characterized by highly variable optical brightness (~3 mag in V band) as well as broad emission lines (e.g., Hα, Hβ, O I at 6300 Å) indicative of active accretion onto the star (Schisano et al. 2009; Kastner et al. 2012). The variability of the optical magnitude, emission line intensities, and extinction measured toward the star are likely associated with a circumstellar disk seen at a relatively high inclination angle; based on modeling of near-infrared interferometric data, Olofsson et al. (2013) estimate that the disk inclination is $i \approx 60°$ (where $i = 90°$ would be edge-on). Such a disk viewing geometry is further supported by the relatively large absorbing column of gas toward the star that is inferred from X-ray spectroscopy ($N_H \approx 10^{22}$ cm^{-2}; Güdel et al. 2010). The spectral energy distribution (SED) of T Cha from optical to millimeter wavelengths has been studied by several authors (Brown et al. 2007; Olofsson et al. 2011, 2013; Cieza et al. 2011). These studies indicate that the T Cha disk has an optically thick inner disk (radius 0.13–0.17 AU) and an outer disk of radius >10 AU (see below) separated by a cavity. Infrared adaptive optics imaging hints at the potential presence of a substellar (perhaps even planetary mass) companion at ~7 AU, which may be responsible for excavating the cavity in the T Cha dust disk (Huélamo et al. 2011); however, a recent reanalysis of these data indicates the excess infrared flux indicative of this close companion may instead be due to anisotropic scattering in the disk (Olofsson et al. 2013). An analysis of the SED from the far-IR to mm-wave shows that the outer disk only extends from 10 to 30 AU, with very little mass outside (Cieza et al. 2011). Line profiles of [Ne II] emission from T Cha, obtained via high spectral resolution mid-IR spectroscopy, indicate that the gaseous component of the inner disk is photoevaporating due to high-energy irradiation by the star (Pascucci & Sterzik 2009; Sacco et al. 2012).

In this paper, we report the detection of submillimeter emission from the circumstellar disk orbiting T Cha in transitions of ^{12}CO, its most abundant isotopologue ^{13}CO, and three other trace molecular species (HCO$^+$, HCN, CN). In Sect. 2, we describe the new submillimeter observations; in Sect. 3 we describe the submillimeter data analysis as well as the properties of X-ray emission from T Cha as determined from a reanalysis of archival data; in Sect. 4 we discuss our results by comparing the properties of the disk around T Cha with the other nearby transition disks TW Hya, V4046 Sgr, and MP Mus; and in Sect. 5 we draw our conclusions.

Table 1. Observation log.

Day (dd-mm-yyyy)	Lines	Time (h)	pwv (mm)
18-09-2011	^{12}CO (3–2), ^{13}CO (3–2)	4.2	0.6–0.8
21-09-2011	^{12}CO (3–2)	2.2	0.3–0.9
22-09-2011	^{12}CO (3–2)	2.2	0.3–0.9
14-05-2012	^{13}CO (3–2)	2.7	0.8–1.1
20-05-2012	^{13}CO (3–2)	5.2	0.6–1.1
21-05-2012	HCO$^+$ (4–3), HCN (4–3)	3.0	0.5–0.7
27-07-2012	HCO$^+$ (4–3), HCN (4–3)	5.3	0.7–1.0
04-08-2012	CN (3–2)	2.2	1.4–1.8
10-08-2012	CN (3–2)	2.8	1.0–1.2
11-08-2012	CN (3–2)	2.0	0.9–1.8

2. Submillimeter observations

We observed T Cha (J2000 coordinates α = 11:57:13.550, δ = −79:21:31.54) with the Atacama Pathfinder Experiment (APEX) 12 m telescope (Güsten et al. 2006) in service mode for a total time of 31.8 h (including overheads) over the course of 11 nights in 2011–2012 (Table 1). The first observation, in 2011 September, yielded detection of ^{12}CO $J = 3 \rightarrow 2$ emission; following this detection, in May, July, and August 2012, we observed (and detected emission from) ^{13}CO $J = 3 \rightarrow 2$, HCO$^+$ $J = 4 \rightarrow 3$, HCN $J = 4 \rightarrow 3$, and CN $J = 3 \rightarrow 2$.

All observations used the SHFI/APEX-2 receiver and XFFTS spectral backend. The half-power beamwidth and main-beam efficiency of the APEX 12 m at the frequency range of the Table 1 observations (330–357 GHz) are $\theta_{mb} \approx 17''$ and $\eta_{mb} \approx 0.73$, respectively[1]. During the first observing run in September 2011, we began by using beam-switching mode with the wobbling secondary for background subtraction. These initial observations yielded detection of circumstellar CO from

[1] See http://www.apex-telescope.org/telescope/efficiency/.

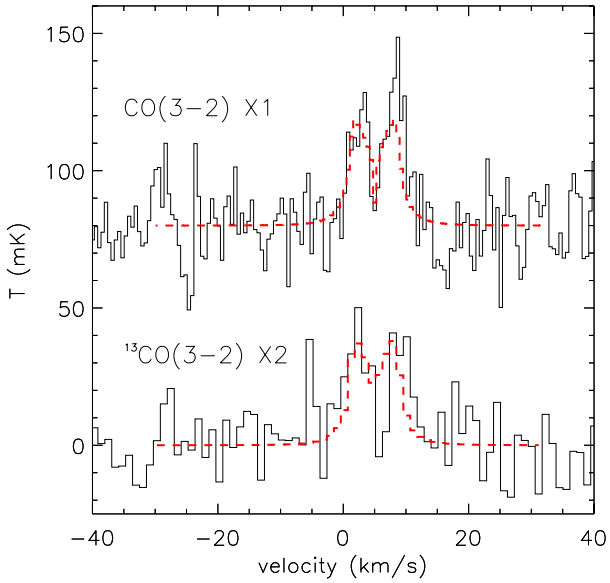

Fig. 1. Observed emission in the ^{12}CO (3–2) and ^{13}CO (3–2) transitions from T Cha. The best fits of the lines with a Keplerian disk model profile are shown with red dashed curves. The ^{13}CO (3–2) intensity is multiplied by a factor 2 and the ^{12}CO (3–2) baseline is offset in temperature to allow a better comparison of the line profiles.

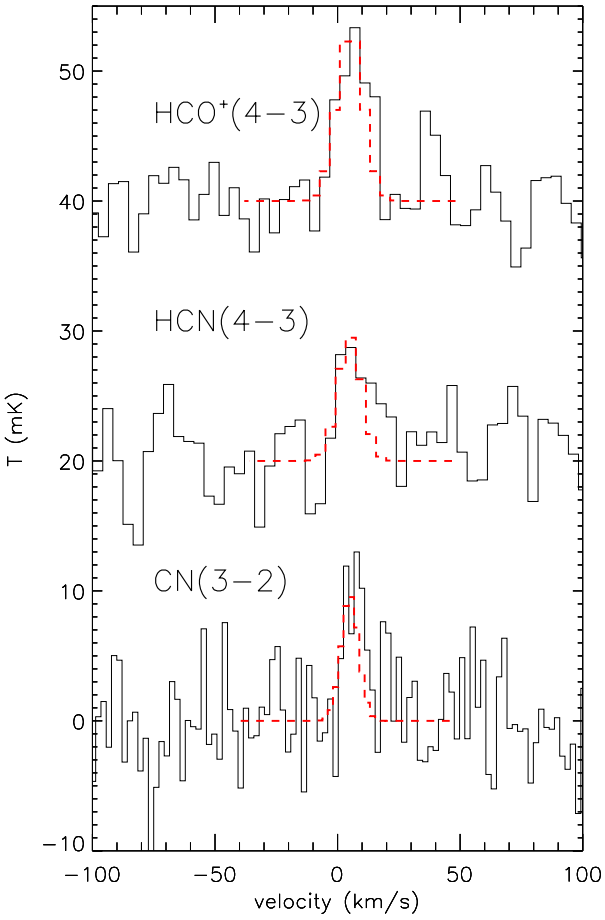

Fig. 2. Observed emission in the HCO$^+$ (4–3), HCN (4–3), and CN (3–2) transitions from T Cha. The best fits of the lines with a gaussian profile are shown with red dashed curves. The baseline of HCO$^+$ (4–3), HCN (4–3) are offset in temperature to provide a better comparison of the line profiles.

T Cha, but with an apparent strong, narrow ^{12}CO "absorption" feature superimposed.

We determined that this narrow CO feature could be attributed to imperfect subtraction of emission from a background molecular cloud (Dcld 300.2–16.9; Nehmé et al. 2008). To properly subtract the emission of the cloud, we used position-switching mode during the second and third nights, taking as reference positions four points offset ∼30″ to the east, west, north, and south of the position of T Cha. This approach allowed us to effectively subtract the cloud emission from the spectrum of circumstellar CO emission. Furthermore, to measure the emission from the cloud, we obtained position-switched spectra, using a distant off-source reference point located well outside the compact cloud. The emission from the cloud is well fitted with a gaussian profile at central velocity $v_{\rm cloud}$ = 4.67 ± 0.02 km s^{-1} (with respect to the local standard of rest, LSR), with a peak temperature $T_{\rm peak}$ = 0.82 ± 0.07 K and $\sigma_{\rm cloud}$ = 0.23 ± 0.02 km s^{-1}. Emission from the cloud did not affect the observations of the other molecular transitions, and therefore during the run performed in 2012, we used beam-switching mode for background subtraction.

3. Data analysis

3.1. Molecular line emission

To reduce and analyze the data, we used the CLASS[2] radio spectral line data reduction package and our own IDL-based analysis tools. Specifically, we used CLASS to co-add spectral scans, correct for the beam efficiency, and subtract baselines, while line fitting was performed by IDL scripts.

In Figs. 1 and 2 we display the results for emission from the T Cha disk in the ^{12}CO (3–2), ^{13}CO (3–2), HCO$^+$ (4–3), HCN (4–3), and CN (3–2) transitions. Although somewhat noisy, the ^{12}CO(3–2) line profile (and, possibly, the ^{13}CO(3–2) line profile) appears to exhibit steep sides and a double-peaked shape, as expected in the case of emission from an orbiting molecular disk (e.g., Beckwith & Sargent 1993). Therefore, we fit the ^{12}CO(3–2) line with a parametric representation of the line profile predicted by a Keplerian disk model, as described in Beckwith & Sargent (1993). This parametric model was used by Kastner et al. (2008, 2010) to analyze the molecular emission detected from V4046 Sgr and MP Mus. The parameters of this model are: the peak temperature $T_{\rm peak}$; the shift of the line centroid with respect to LSR, v_0; the half-value of the velocity separation between the two line peaks $v_{\rm d}$, which is equal to the radial velocity of the outer disk; the slope of the line wings q; and the slope of the central trough between the two peaks p. The q parameter describes the disk radial temperature profile $T \propto r^{-q}$, while p, in the case of an edge-on disk, indicates the definition of the disk outer edge (i.e., for a nearly edge-on disk, p=1 would correspond to a sharp outer edge, and a value $p < 1$ indicates the lack of a sharp edge).

The best-fit parameters and the line fluxes determined from the model (with 1σ errors) are reported in Table 2. To fit the ^{12}CO(3–2) profile, we left all parameters free with the exception of the slope of the outer wings, q, which was fixed to the canonical value 0.5 (Beckwith & Sargent 1993); to fit the ^{13}CO(3–2) line, all parameters with the exception of $T_{\rm peak}$ were kept fixed at the values determined from the best fit to the ^{12}CO(3–2) profile. The velocity of the line centroid (v_0 = 5.03 ± 0.04 km s^{-1}, LSR) determined from the ^{12}CO profile

[2] See http://iram.fr/IRAMFR/GILDAS/

Table 2. Results.

Transition	ν (GHz)	T_{peak} (mK)	v_d (km s^{-1})	q^a	$p_d{}^b$	Flux^c (Jy km s^{-1})
^{12}CO (3–2)	345.796000	38.1 ± 2.3	3.5 ± 0.2^d	0.5	0.27 ± 0.03	12.7 ± 1.2
^{13}CO (3–2)	330.587960	20.0 ± 5.4	3.5^{d,e}	0.5	0.27^e	7.0 ± 2.1
HCO$^+$ (4–3)	356.734242	13.2 ± 3.6	5.5 ± 1.2^f	–	–	7.4 ± 2.5
HCN (4–3)	354.505469	9.5 ± 3.9	4.9 ± 1.6^f	–	–	4.9 ± 2.5
CN (3–2)	340.247781	9.5 ± 3.4	3.6 ± 1.1^f	–	–	3.7 ± 1.6

Notes. Results from the fit of the CO lines with a Keplerian disk model profile (see Sect. 3) and of the other lines with a Gaussian. $^{(a)}$ Power law index of the radial temperature profile within the disk. Fixed at a canonical value. $^{(b)}$ Parameter that describes the outer disk cutoff. $^{(c)}$ Converted from K km s^{-1} to Jy km s^{-1}, using the conversion factor for APEX reported at the website `http://www.apex-telescope.org/telescope/efficiency/`. $^{(d)}$ One half of the differences between red and blue peak velocities. $^{(e)}$ Assumed equal to the value derived from the fit of the ^{12}CO (3–2) line. $^{(f)}$ Standard deviation of the best fit Gaussian.

is in agreement with the radial velocity of T Cha (v_0 = 4.1 ± 1.3 km s^{-1}, after conversion to LSR), as measured by Guenther et al. (2007) via optical spectroscopy. However, our measurement is more accurate, since multiple optical spectroscopic observations of T Cha show that the radial velocity derived from the photospheric absorption lines is variable due to either the presence of a low-mass companion or very strong stellar activity (Schisano et al. 2009). The value of p is consistent with the values determined for the gaseous disks orbiting V4046 Sgr and MP Mus (Kastner et al. 2008, 2010).

Due to the weakness of the line fluxes with respect to the noise, it is not possible to determine reliable Keplerian model parameter values from the line profiles of the other three transitions observed (HCO$^+$, HCN, and CN). Hence, we rebinned these data to coarser spectral resolution and fit all three lines with Gaussians whose central velocity was fixed to the value determined from ^{12}CO, i.e., v_0 = 5.0 km s^{-1}. The resulting best-fit Gaussian parameters and line fluxes (with errors) for HCO$^+$, HCN, and CN are reported in Table 2.

3.2. X-ray emission

The X-ray telescope *XMM-Newton* observed T Cha on March 16, 2009 (ID 0550120601; P.I. M. Güdel). The star was well detected in this observation (as was a candidate wide-separation, low-mass companion; Kastner et al. 2012). Cursory results of spectral analysis performed on the XMM European Photon Imaging Camera (EPIC) detection of T Cha were reported by Güdel et al. (2010). Specifically, they derived an intrinsic 0.3-10 keV X-ray luminosity of $L_X = 1.1 \times 10^{30}$ erg s^{-1} (assuming a distance of 66 pc) and an absorbing column of $N_H = 0.97 \times 10^{22}$ cm^{-2}. Since T Cha lies well in the foreground of the Cha dark clouds (Torres et al. 2008), the large value of N_H determined by Güdel et al. (2010) is evidently dominated by gas in the disk along the line of sight to the star. In light of our detection of cold molecular gas in the T Cha disk, and the likelihood that this cold gas is mainly responsible for the absorption of soft X-rays from T Cha, we have independently reduced and analyzed the archival *XMM-Newton* observation of T Cha, so as to re-examine the determination of N_H and its dependence on assumed X-ray source spectral model parameters.

Standard SAS (v. 11.0) tasks were used to filter events and extract EPIC pn, MOS1, and MOS2 spectra and spectral responses for T Cha. The star was detected with all three instruments, with respective count rates of 0.134, 0.064, and 0.062 counts s^{-1} over effective exposure times of 3.06, 10.07, and 10.67 ks. We used XSPEC (v. 12.6) to fit the filtered 0.15–8.0 keV X-ray spectra with a model consisting of a two-component, optically thin thermal plasma (XSPEC model `vapec`; Smith et al. 2001; Foster et al. 2012) suffering intervening absorption (model `wabs`; Morrison & McCammon 1983). Plasma model abundances were initially uniformly set to 0.8 times solar; this uniform-abundance model yielded an acceptable fit to the EPIC spectra (χ^2 = 1.1 for 140 degrees of freedom) for parameters of $N_H = 1.2 \times 10^{22}$ cm^{-2}, T_1 = 0.8 keV, T_2 = 2.3 keV, and an intrinsic $L_X = 5.1 \times 10^{30}$ erg s^{-1} assuming a distance of 110 pc. However, this model fails to reproduce a strong spectral feature near 1 keV that would appear to be due to a blend of NeIX and NeX emission lines.

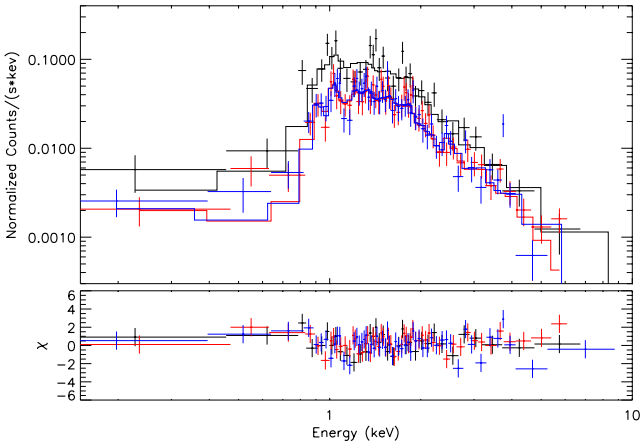

Fig. 3. *Upper panel*: *XMM-Newton* X-ray spectra (crosses) of T Cha filtered between 0.15–8.0 keV. The three colors (black, red, and blue) represent the three detectors (pn, MOS1, and MOS2, respectively) of the instruments for low-resolution spectroscopy on board *XMM-Newton*. The histograms describe the best fit of the data with a model of the absorbed emission from a two-temperature optically thin plasma. *Lower panel*: residuals of the best fit.

Hence, guided by the likelihood that the intrinsic X-ray spectrum of the T Cha source bears a strong resemblance to those of the weakly accreting (and more nearly pole-on) transition disk objects TW Hya (Kastner et al. 2002; Brickhouse et al. 2010) and V4046 Sgr (Günther et al. 2006), we chose a model abundance pattern determined for the former star's X-ray source (specifically, Model C in Brickhouse et al. 2010). The pn and MOS spectra, overlaid with this best-fit model, are displayed in Fig. 3. We find best-fit temperatures of $T_1 = 0.30^{+0.04}_{-0.02}$ keV and $T_2 = 1.8^{+0.4}_{-0.3}$ keV and an intervening absorbing column of $N_H = 1.97^{+0.14}_{-0.15} \times 10^{22}$ cm^{-2}. It would appear that the T Cha EPIC spectra, including the ∼1 keV feature, are well described by this heavily-absorbed but otherwise "TW Hya-like" model

Table 3. Properties of nearby T Tauri star/disk systems.

Star	SpT	$M_\star$ ($M_\odot$)	D (pc)	Age (Myr)	Incl. (°)	$R_{\rm disk,CO}$[a] (AU)	$M_{\rm disk,CO}$[b] ($M_\oplus$)	$M_{\rm disk,H_2}$[b] ($M_\oplus$)	$N_{\rm H}$ (10^{20} cm^{-2})	$M_{\rm disk,Dust}$ ($M_\oplus$)	Ref
T Cha	K0	1.5	110	5–7	60	80	0.08	80	197 ± 15	7	1, 2, 3, 4
MP Mus	K1	1.2	103	7	30	120	0.06[c]	60	4.6 ± 1.8[d]	20	1, 5, 6, 7
V4046 Sgr	K5+K7	1.75[e]	73	12–20	35	370[f]	0.1	100	~2–4[g]	20	8, 9, 10, 11, 12
TW Hya	K7	0.7	54	8	6–7	200[f]	0.02	20[h]	4–30[i]	60	13, 14, 15, 16

Notes. [(a)] Derived from the fit of the ^{12}CO line profile with a Keplerian disk model, using methods and assumptions described in Sect. 4.1, unless otherwise noted. [(b)] Calculated from the ^{13}CO line flux, using methods and assumptions described in Sect. 4.1, unless otherwise noted. [(c)] Calculated from ^{12}CO line flux, assuming the same flux ratio ^{12}CO (3–2)/^{13}CO (3–2) observed for T Cha (i.e. $\tau_{12\rm CO} = 38$). [(d)] Derived from *XMM-Newton* high-resolution spectroscopic observations. [(e)] Total mass of central binary. [(f)] Disk CO radius based on interferometric mapping. [(g)] Range of variability within a one week monitoring. [(h)] Bergin et al. (2013) estimated from the hydrogen deuteride a disk mass three orders of magnitude larger than our estimation from CO. [(i)] Range of values measured from different lines, using high-resolution *Chandra* data.

References. (1) Torres et al. (2008); (2) Olofsson et al. (2011); (3) this work; (4) Cieza et al. (2011); (5) Kastner et al. (2010) and references therein; (6) Argiroffi et al. (2007); (7) Carpenter et al. (2005); (8) Rodriguez et al. (2010); (9) Rosenfeld et al. (2012a) and references therein; (10) Binks & Jeffries (2013); (11) Kastner et al. (2008); (12) Argiroffi et al. (2012); (13) Rosenfeld et al. (2012b) and references therein; (14) Thi et al. (2004); (15) Brickhouse et al. (2010); (16) Thi et al. (2010).

(reduced $\chi^2 = 1.1$ for 140 degrees of freedom). As the precise values of T_1 and $N_{\rm H}$ are somewhat degenerate, their 90% confidence ranges were determined via a two-parameter χ^2 analysis. Although this analysis indicates that the best-fit values are relatively robust, it is important to note that the fit results remain sensitive to the assumed X-ray source atomic abundances (see also discussion in Sect. 4.3).

The foregoing best-fit two-component model with "TW Hya-like" abundances yields integrated (0.15–8.0 keV) observed (absorbed) and intrinsic (unabsorbed) fluxes of $F_{\rm X} = 5.5^{+0.4}_{-1.2} \times 10^{-13}$ erg s^{-1}cm^{-2} and $F_{\rm X,0} = 3.0 \times 10^{-11}$ erg s^{-1} cm^{-2}, respectively, where the large correction from F_X to $F_{\rm X,0}$ is due to the combination of a large $N_{\rm H}$ and the relatively low soft-component temperature (T_1) required for the best model fit. Adopting a distance of 110 pc for T Cha, the value $F_{\rm X,0}$ corresponds to an intrinsic X-ray luminosity of $L_{\rm X} = 4.3 \times 10^{31}$ erg s^{-1}, implying $\log(L_{\rm X}/L_{\rm Bol}) = -2.43$ (given $\log(L_{\rm Bol}/L_\odot) = 0.48$ from Schisano et al. 2009, assuming a distance of 110 pc).

4. Discussion

4.1. Disk structure, mass, and gas/dust ratio

Given some simple assumptions, high spectral resolution observations of circumstellar ^{12}CO and ^{13}CO can be used to estimate the radius of the molecular disk, and the mass contained in the disk (see, e.g., Zuckerman et al. 2008; Kastner et al. 2010, and references therein). Under the assumption of pure Keplerian rotation, we can derive the disk radius from the best-fit value for the outer disk radial velocity ($v_{\rm d}$). Adopting a stellar mass $M = 1.5\ M_\odot$ (Olofsson et al. 2011) and an inclination angle $i = 60°$ (Olofsson et al. 2013), we estimate a disk radius $R_{\rm disk,CO} \sim 80$ AU. As can be noted from Table 3, this result for $R_{\rm disk,CO}$ is similar to (though somewhat smaller than) the radius estimated via similar CO line profile analysis for MP Mus (~120 AU), and is much smaller than the CO disk outer radii measured for V4046 Sgr and TW Hya (~370 and 200 AU, respectively) from interferometric observations of CO (Rodriguez et al. 2010; Qi et al. 2004; Rosenfeld et al. 2012a,b). However, the CO disk radius inferred for T Cha is not as small as its dust disk radius as determined from SED fitting, i.e., $R_{\rm disk,dust} \sim 30$ AU (also assuming $i = 60°$; Cieza et al. 2011). This apparent discrepancy between molecular and dust disk dimensions is similar to that found via interferometric imaging for other similarly evolved disks (e.g., Andrews et al. 2012; Rodriguez et al. 2010; Rosenfeld et al. 2012a). We note that the radii of the molecular disks at V4046 Sgr and TW Hya estimated from their CO line profiles (~250 and 165 AU from Kastner et al. 2008; and Thi et al. 2004, respectively) were both smaller than the radii subsequently measured from interferometers (see preceding paragraph), but still larger than our estimate of the radius of the disk orbiting T Cha.

We estimated the disk mass from the ^{13}CO line flux, using equation A9 in Scoville et al. (1986), which has been used to derive masses of circumstellar disks by Zuckerman et al. (2008) and Kastner et al. (2008, 2010). To obtain the disk CO mass, we assume negligible ^{13}CO optical depth, a CO excitation temperature $T_{\rm ext} \sim 20$ K (as measured for the TW Hya disk, using interferometric observations of CO lines; Qi et al. 2004), a distance $d = 110$ pc (Torres et al. 2008), and an isotopic ratio ^{13}CO/^{12}CO = 69 (appropriate for the local interstellar medium (ISM); Wilson 1999). To convert from CO to H_2 mass, we then adopt a relative CO abundance of [CO]/$H_2 \sim 7 \times 10^{-5}$ (inferred for the Taurus molecular cloud; Dutrey et al. 1997, and references therein).

The resulting disk H_2 gas mass, $M_{\rm disk,H_2} = 2.4 \times 10^{-4}\ M_\odot$ (80 $M_\oplus$), corresponds to a gas to dust mass ratio ~12, adopting the dust mass $M_{\rm dust} = 2.0 \times 10^{-5}\ M_\odot$ derived by Cieza et al. (2011) from SED fitting. If compared with the canonical ISM value ~100, this result would indicate that the circumstellar gas has dissipated faster than the dust component. However, we caution that the foregoing (CO-based) estimated H_2 mass and gas-to-dust mass ratio may be underestimated by a few orders of magnitude, given the uncertainties associated with our many assumptions. Specifically: (a) ^{13}CO may not be optically thin; (b) the ^{13}CO temperature may be lower than 20 K, as this temperature has been estimated from the optically thick ^{12}CO emission that traces the upper, warmer layers of the disk; and (c) the CO abundance is likely $<7 \times 10^{-5}$, due to photodissociation of CO or freeze-out of CO into dust grains.

In Table 3, we compare the foregoing results for the disk gas mass of T Cha with the disk gas (CO and H_2) masses of the other nearby ($d < 100$) accreting T Tauri stars TW Hya, V4046 Sgr, and MP Mus, as recalculated from single-dish measurements

of their submillimeter CO emission[3], using the same method and assumptions[4] as for T Cha. The disk around T Cha has a mass similar to those of the MP Mus and V4046 Sgr disks and about 3.5 times the mass of the TW Hya disk even though, as previously noted, the molecular disk radius estimated from the T Cha line profile is smaller than in the case of the three other, nearby T Tauri star disks listed in Table 3. Therefore, our observations of the gaseous disk component appear to confirm that the disk orbiting T Cha is small and dense, as suggested by Cieza et al. (2011) based on their analysis of mid- to far-IR continuum emission from dust. According to our estimates, the TW Hya disk is less massive and, therefore, less dense than the other disks; this is consistent with its ^{12}CO optical depth, $\tau_{12CO} \sim 13$, which is smaller than the optical depths estimated for T Cha and V4046 Sgr ($\tau_{12CO} \sim 38$ and $\tau_{12CO} \sim 36$, respectively) using the same method. It is interesting that the disk masses of the four stars are correlated with the mass of the central stars, as already observed for the dust masses on a much larger sample of stars (Williams & Cieza 2011). However, more accurate interferometric observations of ^{13}CO (3–2), ^{12}CO, and other isotopologues (i.e., C^{18}O and C^{17}O) are required to better investigate the structures of these circumstellar disks and thereby obtain more accurate estimates of their disk gas masses. Indeed, recent observations of the disks orbiting TW Hya and V4046 Sgr, combined with the results of detailed, self-consistent disk structure and radiative transfer modeling, indicate that their disk H_2 gas masses (i.e., 0.05–0.1 $M_\odot$; Bergin et al. 2013; Rosenfeld et al. 2013) are two to three orders of magnitude larger than the CO-line-based values. Furthermore, in both cases, there are indications of significant variations in gas/dust mass ratio with disk radius (Andrews et al. 2012; Rosenfeld et al. 2013).

4.2. HCN, CN, HCO$^+$ vs. ^{13}CO: comparison with other transition disks

Our detection of T Cha in emission from HCN, CN, and HCO$^+$, in addition to the two CO isotopologues, indicates that the chemical composition of cold gas in the T Cha disk is similar to that of other, similarly evolved disks. Specifically, the relative emission line fluxes we have measured for T Cha in the 0.8 mm regime (see Table 2) are generally similar to those measured for TW Hya and V4046 Sgr in the 1.3 mm and 0.8 mm regimes, respectively (Kastner et al. 1997, 2008), with the exception that T Cha appears to display somewhat weaker CN line emission relative to ^{13}CO (and, as noted by Kastner et al. 2008, TW Hya displays anomalously strong emission from HCO$^+$ relative to ^{13}CO).

Kastner et al. (2008) compared line ratios of HCN, CN, and HCO$^+$ emission with respect to ^{13}CO for a small sample of (mostly) isolated T Tauri disks, finding correlations among the three ratios. These correlations were subsequently confirmed by Salter et al. (2011) on the basis of a larger sample of stars, including young stellar objects in Taurus. Kastner et al. (2008) pointed out that the relative abundances of HCN, CN, and HCO$^+$ are expected to be enhanced in molecular gas that is irradiated by high-energy (ionizing) photons; the fact that TW Hya and V4046 Sgr appear particularly strong in all three of these tracers may then be indicative of their disks' cumulative "doses" of X-ray ionization, due to irradiation by the central stars over their (relatively long) disk lifetimes. Although our results for T Cha are less than definitive in this regard, due to the low significance of our detections of ^{13}CO, HCN, CN, and HCO$^+$, it would appear that T Cha shows a similar pattern of enhanced HCN and HCO$^+$ (if not CN) abundance, indicative of disk X-ray irradiation. Clearly, additional, higher quality measurements of emission from the T Cha disk in these and other potential tracers of disk irradiation are warranted.

4.3. Implications of X-ray spectral analysis

In our X-ray spectral analysis (see Sect. 3.2), we confirm the basic result, previously obtained by Güdel et al. (2010), that the T Cha X-ray source is subject to an intervening absorbing column of order $N_H \sim 10^{22}$ cm^{-2}. We find, furthermore, that the inferred value of N_H is not very sensitive to the adopted intrinsic X-ray source model. This column density is much larger than the values of N_H determined for MP Mus, V4046 Sgr, and TW Hya (see Table 3). This large discrepancy suggests that in stars harboring disks seen at a high inclination angle, like T Cha ($i \approx 60°$), the molecular disk is the main contributor to the X-ray absorption, while in other stars that are viewed more nearly pole-on, like MP Mus, V4046 Sgr, and TW Hya (see Table 3), atomic absorption can be due to material located much closer to the star (e.g., accretion columns connecting the inner disk to the stellar photosphere).

The ratio between atomic absorption and optical extinction $(N_H/A_V)_{TCHA}$ lies in the range $\sim(4-16) \times 10^{21}$ cm^{-2} mag^{-1} ($A_V \sim 1.2-4.6$ mag). This is a factor ~2–7 larger than the ratio $(N_H/A_V)_{ISM}$ observed in the ISM ($(N_H/A_V)_{ISM} \sim 2.2 \times 10^{21}$ cm^{-2} mag^{-1}, Ryter 1996), and larger than ratios observed for young stellar objects in the Orion nebula cluster (Feigelson et al. 2005). The (N_H/A_V) ratio depends on the dust grain properties, but as discussed by Schisano et al. (2009) and Cieza et al. (2011), the dust grains within the T Cha disk are larger than ISM grains; hence, the extinction curve is flatter than characteristic of the ISM (i.e., $R_v \sim 5.5$ for T Cha; Schisano et al. 2009) and, as a result, we would expect the (N_H/A_V) ratio to be lower than the ISM value (Draine 2003). Thus, the relatively large value of $(N_H/A_V)_{TCHA}$ appears to indicate that the fraction of metals in the gas phase is higher than in the dust phase, since metals (especially C, N, and O) are the main contributors to X-ray absorption (Morrison & McCammon 1983; Vuong et al. 2003).

We caution, however, that the standard X-ray absorption model we and others employ to determine N_H has been developed for physical conditions appropriate to the ISM (e.g., 20% of H in molecular form; Wilms et al. 2000). Hence, application of this same ISM-based model to the evolved circumstellar disk orbiting T Cha, in which the gas is likely predominantly molecular, and the gas/dust mass ratio may vary significantly along the line of sight (e.g., Andrews et al. 2012; Rosenfeld et al. 2013), implies there may be large systematic uncertainties in the results for N_H. Development of an X-ray absorption model appropriate for the molecular-to-atomic gas fractions and molecular abundances characteristic of circumstellar disks would reduce these uncertainties, although such an effort is clearly beyond the scope of this paper.

[3] For these disk mass calculations, we used the ^{13}CO (3–2) and ^{13}CO (2–1) line fluxes for TW Hya and V4046 Sgr, respectively; while for MP Mus, we estimated the ^{13}CO (3–2) flux from the measured ^{12}CO (3–2) line flux, assuming the same ^{13}CO (3–2)/^{12}CO (3–2) ~ 1.8 flux ratio observed for T Cha, which corresponds to an optical depth $\tau_{12CO} \sim 38$ under the assumption that the ^{13}CO (3–2) emission is optically thin.

[4] Values reported in Table 3 are slightly different from the values reported in Kastner et al. (1997, 2008, 2010) due to different assumptions for gas temperature, ^{12}CO/^{13}CO isotopic ratio, CO optical thickness, and CO abundance.

Significantly, given the assumption that the abundance patterns in X-ray-emitting plasma are "TW Hya-like", the X-ray spectral model fitting provides evidence for the presence of a soft plasma component, with characteristic temperature $T_X \sim 3.5 \times 10^6$ K. A similarly soft plasma component has been observed in several classical (actively accreting) T Tauri stars. The most notable examples are the other three stars in Table 3, i.e., TW Hya, V4046 Sgr, and MP Mus (Kastner et al. 2002; Argiroffi et al. 2007, 2012). As in these cases, the presence of such a component in the T Cha X-ray spectrum could be indicative of soft X-ray emission produced by shocks at the base of accretion columns.

On the other hand, as a consequence of the large inferred value of N_H, the intrinsic X-ray luminosity implied by the presence of such a soft component would make T Cha unusually X-ray luminous among T Tauri stars. Specifically, our model fitting implies $\log(L_X/L_{Bol}) = -2.43$, i.e., roughly an order of magnitude larger than typical of T Tauri stars (e.g., Kastner et al. 2012, and references therein). Again, however, we caution that the inference of luminous, soft X-ray emission from T Cha rests in large part on the accuracy of the model describing X-ray absorption within its circumstellar disk. Furthermore, as discussed in Brickhouse et al. (2010) and Sacco et al. (2010), any soft component attributed to accretion shocks may be affected by chromospheric absorption, depending on the location of the post-shock zone. X-ray gratings spectroscopy observations of T Cha are therefore required to more conclusively demonstrate the presence of accretion-shock-generated X-ray emission from the star.

Interestingly, our X-ray spectral fitting results are very similar to those obtained by Skinner & Güdel (2013) for the transition disk system LkCa 15, which, like T Cha, is viewed at relatively high inclination ($i \approx 50°$; Piétu et al. 2007). In particular, both the T Cha and LkCa 15 X-ray spectral analyses reveal evidence for a "cool" ($T_X \sim 3 \times 10^6$ K) plasma component that dominates the total X-ray flux but is heavily absorbed, due (presumably) to intervening disk material.

5. Conclusions

We have performed a series of submm observations of T Cha with the APEX 12 m radiotelescope, and we reanalyzed the available *XMM-Newton* archival X-ray data for this star, with the aim of studying the physical and chemical properties of its circumstellar disk. We obtained the following main results:

1. We detected molecular emission from the T Cha disk, providing the first evidence for the presence of cold gas out to large radii from the star (i.e., >10 AU). Specifically, we detected and measured the fluxes of the ^{12}CO (3–2), ^{13}CO (3–2), HCO$^+$ (4–3), HCN (4–3), and CN (3–2). The ^{12}CO (3–2) line profile (and, possibly, ^{13}CO (3–2) line profile) is double-peaked, indicative of Keplerian rotation.
2. T Cha joins TW Hya, V4046 Sgr, and MP Mus as the fourth nearby ($D \lesssim 100$ pc) classical T Tauri star of roughly solar mass and age of at least ~5 Myr, which is known to harbor a molecular disk. Its detection in radio molecular line emission further strengthens the connection between the presence of a cold, gaseous disk and signatures of stellar accretion, even in stars in an advanced stage of the pre-MS phase (Kastner et al. 2010).
3. From a parametric fit of a Keplerian disk model line profile to the measured ^{12}CO (3–2) line profile, we find an outer disk projected rotational velocity of $v_d = 3.5$ km s^{-1}. Under the assumption of pure Keplerian rotation and a disk inclination angle $i = 60°$, this value of v_d implies an outer disk radius $R_{disk,CO} \sim 80$ AU. This CO disk radius is smaller than the radii measured interferometrically for other, similar transition disks, such as TW Hya and V4046 Sgr. However, the CO radius we infer for the T Cha disk is significantly larger than the dust disk radius previously deduced from its infrared SED. Submillimeter interferometric observations of T Cha that can provide direct measurements of the disk's geometrical properties are clearly warranted.
4. From the ^{13}CO (3–2) line flux, we estimate a total disk gas mass $M_{disk,H_2} \sim 80\ M_\oplus$ and a gas-to-dust mass ratio ~12, where the latter is based on a disk dust mass estimate from the literature (Cieza et al. 2011). These values are similar to those obtained for other disks of similar age. However, we caution that such (single-dish, CO-based) estimates may suffer from large uncertainties, most of which may lead to severe underestimates in disk gas mass.
5. From a reanalysis of archival *XMM-Newton* X-ray observations, we find T Cha has an intrinsic X-ray luminosity $L_X = 4.3 \times 10^{31}$ erg s^{-1}, with an intervening atomic absorbing column of $N_H = 2.0 \times 10^{22}$ cm^{-2}. The X-ray spectral analysis yields evidence for a strong soft component, possibly indicative of accretion shocks. The relatively large value of N_H is indicative of absorption due to intervening gas that resides in the (highly inclined) T Cha disk. The resulting inferred ratio between atomic absorption and visual extinction for the T Cha disk lies in the range $N_H/A_V \approx 4$–16×10^{21} cm^{-2}. This is somewhat larger than the N_H/A_V ratios characteristic of the ISM and star-forming clouds, indicating that the disk gas is rich in metals. However, an X-ray absorption model appropriate for the physical and chemical conditions of a circumstellar disk is required to address this issue.
6. The intensities of HCO$^+$ and HCN emission relative to ^{13}CO measured for T Cha are similar to the relative HCO$^+$ and HCN line intensities of the (similarly evolved) disks orbiting TW Hya and V4046 Sgr. The relative intensity of CN line emission appears somewhat weaker in the case of T Cha, but due to the low signal-to-noise ratio of our detection, this discrepancy is not strongly significant. Additional, more sensitive measurements of the T Cha disk in these tracers may clarify whether the disk displays chemical signatures of the ionizing effects of X-ray irradiation, as would be expected given the clear indications, from *XMM-Newton* X-ray spectroscopy, of a large X-ray absorbing column due to intervening disk material.

Acknowledgements. We would like to thank the anonymous referee for useful and constructive comments and S. Murphy for the discussion about the distance and the age of T Cha. This publication is based on data acquired with the Atacama Pathfinder Experiment (APEX). APEX is a collaboration between the Max-Planck-Institut fur Radioastronomie, the European Southern Observatory, and the Onsala Space Observatory. This research was supported in part by US National Science Foundation grant AST-1108950 to RIT.

References

Alencar, S. H. P., & Batalha, C. 2002, ApJ, 571, 378
Andrews, S. M., Wilner, D. J., Hughes, A. M., et al. 2012, ApJ, 744, 162
Argiroffi, C., Maggio, A., & Peres, G. 2007, A&A, 465, L5
Argiroffi, C., Maggio, A., Montmerle, T., et al. 2012, ApJ, 752, 100
Beckwith, S. V. W., & Sargent, A. I. 1993, ApJ, 402, 280
Bergin, E. A., Cleeves, L. I., Gorti, U., et al. 2013, Nature, 493, 644
Binks, A. S., & Jeffries, R. D. 2013, MNRAS, in press
Brickhouse, N. S., Cranmer, S. R., Dupree, A. K., Luna, G. J. M., & Wolk, S. 2010, ApJ, 710, 1835
Brown, J. M., Blake, G. A., Dullemond, C. P., et al. 2007, ApJ, 664, L107

Carpenter, J. M., Wolf, S., Schreyer, K., Launhardt, R., & Henning, T. 2005, AJ, 129, 1049
Cieza, L. A., Olofsson, J., Harvey, P. M., et al. 2011, ApJ, 741, L25
Curran, R. L., Argiroffi, C., Sacco, G. G., et al. 2011, A&A, 526, A104
Draine, B. T. 2003, ARA&A, 41, 241
Dutrey, A., Guilloteau, S., & Simon, M. 1994, A&A, 286, 149
Dutrey, A., Guilloteau, S., & Guelin, M. 1997, A&A, 317, L55
Dutrey, A., Guilloteau, S., Piétu, V., et al. 2008, A&A, 490, L15
Feigelson, E. D., Getman, K., Townsley, L., et al. 2005, ApJS, 160, 379
Foster, A. R., Ji, L., Smith, R. K., & Brickhouse, N. S. 2012, ApJ, 756, 128
Güdel, M., Lahuis, F., Briggs, K. R., et al. 2010, A&A, 519, A113
Guenther, E. W., Esposito, M., Mundt, R., et al. 2007, A&A, 467, 1147
Günther, H. M., Liefke, C., Schmitt, J. H. M. M., Robrade, J., & Ness, J.-U. 2006, A&A, 459, L29
Güsten, R., Nyman, L. Å., Schilke, P., et al. 2006, A&A, 454, L13
Huélamo, N., Lacour, S., Tuthill, P., et al. 2011, A&A, 528, L7
Hughes, A. M., Wilner, D. J., Andrews, S. M., Qi, C., & Hogerheijde, M. R. 2011, ApJ, 727, 85
Kastner, J. H., Zuckerman, B., Weintraub, D. A., & Forveille, T. 1997, Science, 277, 67
Kastner, J. H., Huenemoerder, D. P., Schulz, N. S., Canizares, C. R., & Weintraub, D. A. 2002, ApJ, 567, 434
Kastner, J. H., Zuckerman, B., Hily-Blant, P., & Forveille, T. 2008, A&A, 492, 469
Kastner, J. H., Hily-Blant, P., Sacco, G. G., Forveille, T., & Zuckerman, B. 2010, ApJ, 723, L248
Kastner, J. H., Thompson, E. A., Montez, R., et al. 2012, ApJ, 747, L23
Morrison, R., & McCammon, D. 1983, ApJ, 270, 119
Murphy, S. J., Lawson, W. A., & Bessell, M. S. 2013, MNRAS, 435, 1325
Nehmé, C., Gry, C., Boulanger, F., et al. 2008, A&A, 483, 471
Öberg, K. I., Qi, C., Fogel, J. K. J., et al. 2010, ApJ, 720, 480
Öberg, K. I., Qi, C., Fogel, J. K. J., et al. 2011, ApJ, 734, 98
Olofsson, J., Benisty, M., Augereau, J.-C., et al. 2011, A&A, 528, L6
Olofsson, J., Benisty, M., Le Bouquin, J.-B., et al. 2013, A&A, 552, A4
Pascucci, I., & Sterzik, M. 2009, ApJ, 702, 724
Piétu, V., Dutrey, A., & Guilloteau, S. 2007, A&A, 467, 163
Qi, C., Ho, P. T. P., Wilner, D. J., et al. 2004, ApJ, 616, L11
Qi, C., Wilner, D. J., Calvet, N., et al. 2006, ApJ, 636, L157
Qi, C., Wilner, D. J., Aikawa, Y., Blake, G. A., & Hogerheijde, M. R. 2008, ApJ, 681, 1396
Rodriguez, D. R., Kastner, J. H., Wilner, D., & Qi, C. 2010, ApJ, 720, 1684
Rosenfeld, K. A., Andrews, S. M., Wilner, D. J., & Stempels, H. C. 2012a, ApJ, 759, 119
Rosenfeld, K. A., Qi, C., Andrews, S. M., et al. 2012b, ApJ, 757, 129
Rosenfeld, K. A., Andrews, S. M., Wilner, D. J., Kastner, J. H., & McClure, M. K. 2013, ApJ, submitted
Ryter, C. E. 1996, Ap&SS, 236, 285
Sacco, G. G., Orlando, S., Argiroffi, C., et al. 2010, A&A, 522, A55
Sacco, G. G., Flaccomio, E., Pascucci, I., et al. 2012, ApJ, 747, 142
Salter, D. M., Hogerheijde, M. R., van der Burg, R. F. J., Kristensen, L. E., & Brinch, C. 2011, A&A, 536, A80
Schisano, E., Covino, E., Alcalá, J. M., et al. 2009, A&A, 501, 1013
Scoville, N. Z., Sargent, A. I., Sanders, D. B., et al. 1986, ApJ, 303, 416
Skinner, S. L., & Güdel, M. 2013, ApJ, 765, 3
Smith, R. K., Brickhouse, N. S., Liedahl, D. A., & Raymond, J. C. 2001, ApJ, 556, L91
Thi, W.-F., van Zadelhoff, G.-J., & van Dishoeck, E. F. 2004, A&A, 425, 955
Thi, W., Mathews, G., Ménard, F., et al. 2010, A&A, 518, L125
Torres, C. A. O., Quast, G. R., Melo, C. H. F., & Sterzik, M. F. 2008, in Young Nearby Loose Associations, ed. B. Reipurth, 757
Vuong, M. H., Montmerle, T., Grosso, N., et al. 2003, A&A, 408, 581
Williams, J. P., & Cieza, L. A. 2011, ARA&A, 49, 67
Wilms, J., Allen, A., & McCray, R. 2000, ApJ, 542, 914
Wilson, T. L. 1999, Rep. Prog. Phys., 62, 143
Zuckerman, B., Forveille, T., & Kastner, J. H. 1995, Nature, 373, 494
Zuckerman, B., Melis, C., Song, I., et al. 2008, ApJ, 683, 1085